Influence of Intramolecular Hydrogen Bond Strength on OH-Stretching Overtones

Daryl L. Howard and Henrik G. Kjaergaard*

Department of Chemistry, University of Otago, P.O. Box 56, Dunedin, New Zealand

Received: June 11, 2006

Vapor-phase OH-stretching overtone spectra of 1,3-propanediol and 1,4-butanediol were recorded and compared to the spectra of ethylene glycol to investigate the effect of increased intramolecular hydrogen bond strength on OH-stretching overtone transitions. The spectra were recorded with laser photoacoustic spectroscopy in the second and third OH-stretching overtone regions. The room-temperature spectra of each molecule are dominated by two conformers that show intramolecular hydrogen bonding. Anharmonic oscillator local-mode calculations of the OH-stretching transitions have been performed to aid assignment of the different conformers in the spectra and to illustrate the effect of the intramolecular hydrogen bonding. The hydrogen bond strength increases in the order ethylene glycol, 1,3-propanediol, and 1,4-butanediol. The overtone transitions of the hydrogen-bonded hydroxyl groups are more difficult to observe with increasing intramolecular hydrogen bond strength. We suggest that the bandwidth of these transitions increases with increasing hydrogen bond strength and with increasing overtone and furthermore that these changes are in part responsible for the lack of observed overtone spectra for complexes.

Introduction

The absorption of solar radiation by hydrogen-bonded complexes in the Earth's atmosphere is significant to climate change.[1−6] Knowledge of the spectroscopy of these complexes, particularly those containing water, is crucial in the assessment of their atmospheric importance.[3−5] The prototypical hydrated complex, water dimer, has possibly been observed in the atmosphere.[6] The band observed corresponded to the third overtone of the donor-bonded OH-stretching mode.[6] However, subsequent laboratory experiments have failed to observe this overtone transition in water dimer,[7] and it has been suggested that the observed ∼20 cm^{-1} width of this transition should be significantly wider.[8] To our knowledge, there are no other observed OH-stretching overtone spectra of hydrated complexes at atmospherically relevant conditions.

The low intrinsic intensity of OH-stretching overtone transitions compounded with the small equilibrium constants of the complexes and low vapor pressures of the monomers makes spectroscopic studies difficult under atmospherically relevant conditions.[9] Alternatively, the effects of hydrogen bonding can be investigated in molecules which contain intramolecular hydrogen bonds, thereby removing the problem of small abundances of complexes. The intramolecular hydrogen bond has been well-studied spectroscopically in the condensed phase;[10,11] however, vapor-phase studies have been limited. Our aim is to observe the effects that increasing hydrogen bond strength have on the OH-stretching overtone spectra of ethylene glycol (EG), 1,3-propanediol (PD), and 1,4-butanediol (BD) under conditions at or near room temperature and to present a possible explanation for the lack of overtone spectra of hydrated complexes.

In the vapor-phase infrared spectrum of EG, both the hydrogen-bonded and free OH-stretching transitions were observed.[12] However, the infrared spectrum was too congested to observe different conformers. This congestion was lifted in the OH-stretching overtone spectrum, and the two lowest-energy conformers were clearly identified.[13] Spectral and theoretical signatures of hydrogen bonding were shown in both EG conformers.[13] The existence of an intramolecular hydrogen bond in EG had been a widely discussed theoretical topic.[14−16]

The extra methylene groups in PD and BD relative to ethylene glycol allow these molecules to adopt increasingly more favorable intramolecular hydrogen-bonding geometries, thereby increasing the strength of the hydrogen bond. Previous studies of PD include ab initio geometry optimizations of its 25 unique conformers at the Hartree−Fock level.[17,18] From these calculations, it was determined that the two lowest-energy conformers had an intramolecular hydrogen bond. The infrared spectrum of vapor-phase PD has been recorded in the OH-stretching region with a 20 cm path length and with a temperature range of 130−170 °C.[19] Bands corresponding to the free and intramolecular hydrogen-bonded OH-stretching vibrations were observed. In both the free and bonded regions, two closely overlapping peaks were observed and assigned to the two lowest-energy conformers.[19] Further evidence of an intramolecular hydrogen-bond conformation in vapor-phase PD was found in an electron diffraction study.[20] In a free-jet microwave absorption spectrum of PD, the most abundant conformer was determined to adopt a six-membered-ring chair conformation similar to the conformer PD**1** shown in Figure 1.[21] The "free" hydroxyl hydrogen was found to be trans to the adjacent C−C bond.[21]

Relative to PD, there are even fewer spectroscopic and theoretical studies on BD. Two vapor-phase infrared spectral studies of gas-phase BD have been reported in the literature.[22,23] Both of these studies were concerned with hydrogen-bonding effects in solution, and neither the vapor-phase spectra nor the corresponding OH-stretching peak positions were given. Intramolecular hydrogen-bonded conformers of BD were found to be dominant at 144 and 260 °C in an electron diffraction study.[24] Initial theoretical calculations at the CNDO/2 level[25] and at the molecular mechanics level[24] have been followed up by a more

* E-mail: henrik@alkali.otago.ac.nz.

10.1021/jp063631+ CCC: $33.50
Published on Web 08/05/2006

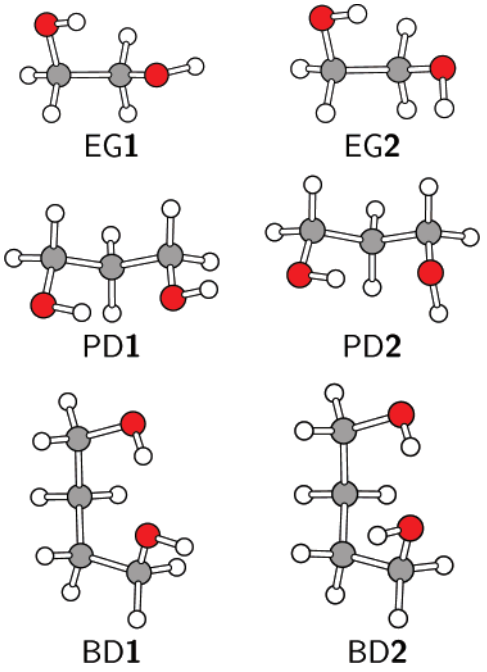

Figure 1. The two lowest-energy conformers of ethylene glycol (EG), 1,3-propanediol (PD), and 1,4-butanediol (BD).

comprehensive study, in which the lowest-energy structures were first systematically obtained from a molecular mechanics conformational search.[26] The structures with an energy less than 10 kJ mol^{-1} above the global minimum were reoptimized at the B3LYP/6-311++G(d,p) level. The two most stable conformers were both intramolecular hydrogen-bonded forms, with calculated populations of 51% and 27% at room temperature.[26] These calculated populations of BD are similar to those calculated for the two intramolecular hydrogen-bonded conformers of EG.[13,27]

The vapor-phase overtone spectra of PD and BD have not previously been recorded. However, the first OH-stretching overtone regions of PD and BD have been recorded in a dilute CCl_4 solution.[28] The reported red shifts of the bonded OH_b-stretching transitions compared to the free OH_f-stretching transitions in PD and BD are 166 and ~236 cm^{-1}, respectively.[28]

In the present paper, the vapor-phase spectra of PD and BD have been recorded in the second and third OH-stretching overtone regions and compared with our previous spectra of EG.[13] Geometry optimizations of the two lowest-energy conformers of these three diols have been performed at the quadratic configuration interaction including singles and doubles (QCISD) levels of theory with the 6-311++G(2d,2p) basis set. Anharmonic oscillator local-mode calculations[13,29] have been performed to calculate the OH-stretching spectra. The necessary local-mode frequencies and anharmonicities of the OH-stretching vibrations as well as the dipole-moment functions were calculated with the QCISD/6-311++G(2d,2p) method. It was shown for EG that the local-mode model combined with calculations at the CCSD(T)/aug′-cc-pVTZ level (where aug′ indicated augmentation only on the OH groups) could accurately predict the observed spectra.[13] Unfortunately, it is not possible to run CCSD(T)/aug′-cc-pVTZ calculations for PD and BD. Calculations at the less computationally expensive QCISD/6-311++G(2d,2p) level are possible for all three diols, and we compare with the CCSD(T) calculations for EG as a benchmark. The anharmonic oscillator calculations for the three diols will facilitate assignment of the PD and BD spectra. The combination of observed spectra and calculations for the series EG, PD, and BD will allow us to assess the effect on OH-stretching overtone transitions of increased intramolecular hydrogen-bonding strength.

Experimental Section

The samples of 1,3-propanediol (Merck-Schuchardt, 98%) and 1,4-butanediol (Aldrich, 99+%) were not further purified except for degassing and drying as described previously for ethylene glycol.[13]

The second and third OH-stretching overtone regions (Δv_{OH} = 3 and 4) of PD and BD were recorded with intracavity laser photoacoustic spectroscopy. Our photoacoustic spectrometer and the spectral calibration process have been described previously.[30] Briefly, a Coherent Innova Sabre argon ion laser running at all lines was used to pump a Coherent 890 titanium:sapphire laser. The wavelength is tuned with a three-plate birefringent filter which yields a laser line width of approximately 1 cm^{-1}. The photoacoustic cell contained a Knowles EK3133 microphone for detection of the photoacoustic signal. The spectra of EG and PD were recorded at 20 °C, and the spectra of BD at 40 °C. The BD sample was heated as described previously for EG.[13] The photoacoustic signal was enhanced by the addition of a buffer gas of 200 Torr argon to the photoacoustic cell for all the spectra.[31,32]

Vibrational Theory. We have used an anharmonic oscillator local-mode model to describe the OH-stretching modes.[33,34] The details of this model are given in a recent paper.[13] The vibrational Hamiltonian is approximated by a Morse oscillator and the dipole-moment function as a series expansion in the internal displacement coordinate q. The local-mode frequency $\tilde{\omega}$ and anharmonicity $\tilde{\omega}x$ and the dipole-moment series expansion coefficients are determined from ab initio calculated potential energy and dipole-moment curves. The grid points in the curves are calculated by serially displacing q by ±0.2 Å from equilibrium in steps of 0.05 Å for a total of nine points. We have limited the series expansion of the dipole moment to the fifth order.[35,36] The OH-stretching frequency and anharmonicity are obtained from the second-, third-, and fourth-order derivatives of the potential energy with respect to the OH-stretching coordinate according to the equations given previously.[13] These derivatives are determined by fitting an eighth order polynomial to the nine-point grid. Intensities are expressed in the dimensionless oscillator strength f.

The geometry optimizations and all grid points are calculated with the QCISD/6-311++G(2d,2p) method. The ab initio calculations were performed with *MOLPRO*.[37]

Results and Discussion

Diol Geometries. We have previously used the anharmonic local-mode model combined with the CCSD(T)/aug′-cc-pVTZ method to successfully calculate the OH-stretching vibrational spectra of the different conformers of EG.[13] As mentioned, both PD and BD are too large to model with this CCSD(T) method, and we have instead used the QCISD/6-311++G(2d,2p) method to model the OH-stretching spectra of the two lowest-energy conformers of the three diols. We expect that the QCISD/6-311++G(2d,2p) method will reveal the trends pertaining to the hydrogen bonding in the diols, without providing the spectroscopic accuracy obtained at the CCSD(T) level.

The two lowest-energy structures of each of the three diols are shown in Figure 1 with the lowest-energy structure of each diol labeled as **1**. The main structural difference between the two hydrogen-bonded conformers of each diol is the dihedral angle of the "free" hydroxyl group. The intramolecular hydrogen bond geometries in EG, PD, and BD correspond to five-, six-,

TABLE 1: Optimized Geometric Parameters of the Two Lowest-Energy Conformers of 1,2-Ethanediol, 1,3-Propanediol, and 1,4-Butanediol (Å and deg)[a]

conformer	rOH_b	rOH_f	r_{HB}	∠HB
EG**1**	0.9587	0.9555	2.3605	107.5
EG**2**	0.9593	0.9573	2.3599	110.6
PD**1**	0.9593	0.9561	2.0452	137.5
PD**2**	0.9597	0.9577	2.0856	137.1
BD**1**	0.9614	0.9569	1.8924	154.5
BD**2**	0.9616	0.9574	1.9001	153.7

[a] Calculated at the QCISD/6-311++G(2d,2p) level.

and seven-membered quasi-rings, respectively. The lowest-energy structure for PD is consistent with the electron diffraction and microwave results.[20,21]

The QCISD/6-311++G(2d,2p) calculated geometric parameters relating to the hydroxyl groups are presented in Table 1. The labels used are as follows: rOH_b and rOH_f are the bonded and free OH bond lengths, respectively; r_{HB} is the hydrogen bond length, defined as the distance between the acceptor oxygen atom and the donor hydrogen atom, and ∠HB is the hydrogen bond angle, i.e., the $O-H_b\cdots O$ angle. The OH_b bond lengths are calculated to be similar for EG and PD, while they are slightly longer for BD. The calculated hydrogen bond length r_{HB} becomes significantly shorter with increasing diol chain length with distances of approximately 2.4, 2.1, and 1.9 Å. The hydrogen bond angle approaches a more favorable linear geometry in the diols sequence, with calculated angles of approximately 110°, 137°, and 154°. These geometric changes respectively suggest increased intramolecular hydrogen bond strength from EG to PD to BD.[38]

The QCISD/6-311++G(2d,2p)-calculated electronic energy difference between the EG**1** and EG**2** structures is 2.17 kJ mol^{-1} (181 cm^{-1}), in reasonable agreement with the CCSD(T)/aug′-cc-pVTZ value of 1.34 kJ mol^{-1} (112 cm^{-1}).[13] In EG, we found that the zero-point vibrational energy correction increases the energy difference by approximately 0.36 kJ mol^{-1} (30 cm^{-1}). The calculated energy differences for the two lowest-energy structures of PD and BD are 0.95 kJ mol^{-1} (79 cm^{-1}) and 0.98 kJ mol^{-1} (82 cm^{-1}), respectively. The QCISD calculated electronic energy differences are without zero-point vibrational energy correction as this is expected to to alter energies little for the two lowest-energy structures. The structural degeneracy for all conformers in Figure 1 is four and does not alter their relative abundances. Thus, on the basis of these relative energies, the relative abundances of conformers **1** and **2** at both 20 and 40 °C is on the order of 2 to 1.

Anharmonic Oscillator Calculations. The calculated red shifts $\Delta\tilde{\nu}$, defined as the wavenumber difference between the free and hydrogen-bonded OH-stretching transitions and the relative intensities of bonded to free transitions f_b/f_f are shown in Table 2. The calculated local-mode parameters, transition wavenumbers, and oscillator strengths are presented as Supporting Information. A trend of greater red shifts is calculated for the EG to BD sequence. The QCISD-calculated red shifts in the fundamental region compare well to the observed vapor-phase fundamental red shifts of approximately 33, 58, and 110 cm^{-1} for EG,[12] PD,[19] and BD.[22] Unlike the infrared spectrum, the bands associated with the two lowest-energy conformers of EG are observed in the overtone spectra, and a more detailed comparison is possible.[13] The QCISD-calculated red shifts for EG are an underestimate of the observed red shifts in the $\Delta v_{OH} = 3-5$ regions (Supporting Information). In the $\Delta v_{OH} = 5$ region, the red shift is underestimated by about 100 cm^{-1}. The agreement is better with the CCSD(T)/aug′-cc-pVTZ method, which approximately halves the discrepancy.[13]

TABLE 2: Calculated Red Shifts (cm^{-1}) and Relative Intensities in Ethylene Glycol, 1,3-Propanediol, and 1,4-Butanediol[a]

	EG**1**		PD**1**		BD**1**	
v	$\Delta\tilde{\nu}$	f_b/f_f	$\Delta\tilde{\nu}$	f_b/f_f	$\Delta\tilde{\nu}$	f_b/f_f
1	39	1.2	44	4.4	105	9.8
2	77	0.65	89	0.36	227	0.15
3	112	0.63	133	0.46	365	0.34
4	145	0.75	178	0.69	520	0.78
5	177	0.96	223	1.0	691	1.4
	EG**2**		PD**2**		BD**2**	
v	$\Delta\tilde{\nu}$	f_b/f_f	$\Delta\tilde{\nu}$	f_b/f_f	$\Delta\tilde{\nu}$	f_b/f_f
1	22	1.6	36	4.1	92	11.2
2	41	0.76	74	0.43	200	0.22
3	58	0.74	114	0.59	321	0.50
4	73	0.83	157	0.85	455	1.0
5	85	0.97	201	1.1	605	1.6

[a] Calculated with QCISD/6-311++G(2d,2p) local-mode parameters and dipole-moment functions.

The general intensity trend of hydrogen bonding, with stronger f_b for the fundamental[39] and weaker f_b for the first overtone[40] compared to f_f, was calculated for all the diols. In the fundamental, the calculated relative intensities are approximately equal for EG, a factor of 4 greater for PD and an order of magnitude greater for BD. Conversely in the first OH-stretching overtone, f_b becomes increasingly weaker relative to f_f in the EG to BD series. As the vibrational overtone level increases, f_b is calculated to steadily increase relative to f_f. The decrease in intensity of f_b at the first overtone is attributable to a cancellation of terms in the dipole-moment expansion.[41,42] There is not yet a standard criterion for determining the absolute strength of intramolecular hydrogen bonds; however, the intensity trend calculated for the fundamental transitions does suggest a significantly stronger intramolecular hydrogen bond for BD relative to EG.

Observed Overtone Spectra. For each of the diols, we have labeled the OH_b- and OH_f-stretching transitions of conformer **1** as **1**b and **1**f and likewise **2**b and **2**f for conformer **2**.

The vapor-phase OH-stretching overtone spectra of the three diols in the $\Delta v_{OH} = 3$ and 4 regions are presented in Figures 2 and 3, respectively. The **1**f and **2**f transitions of each diol are clearly observed between 10 400 and 10 600 cm^{-1} in the $\Delta v_{OH} = 3$ region and between 13 500 and 13 800 cm^{-1} in the $\Delta v_{OH} = 4$ region. In all spectra, the **1**f band is the most intense. The calculated **2**f transition intensities are approximately 10−15% weaker than the **1**f transitions, and in combination with the relative abundances of the conformers, this leads to the expected relative intensities of approximately 2 to 1 for **1**f to **2**f, in good agreement with the observed relative intensities.

The observed wavenumbers of the **1**f (**2**f) transition of PD and BD are similar, as shown in Figures 2 and 3. The splitting between the **1**f and **2**f transitions is less for PD and BD than for EG. This observation can be attributed to the lower steric hindrance present in the larger diols relative to EG. The similarity in the free transition wavenumbers also indicates that the free hydroxyls are unaffected by increasing intramolecular hydrogen bond strength.

It is immediately apparent from Figures 2 and 3 that the bonded transitions become significantly less distinct in the EG to BD sequence. The bonded transitions **1**b and **2**b in the $\Delta v_{OH} = 3$ EG spectrum are relatively intense and clearly identified. In the $\Delta v_{OH} = 3$ PD spectrum, a weak band is observed at 10 275 cm^{-1}, which we assign to the bonded transitions. We

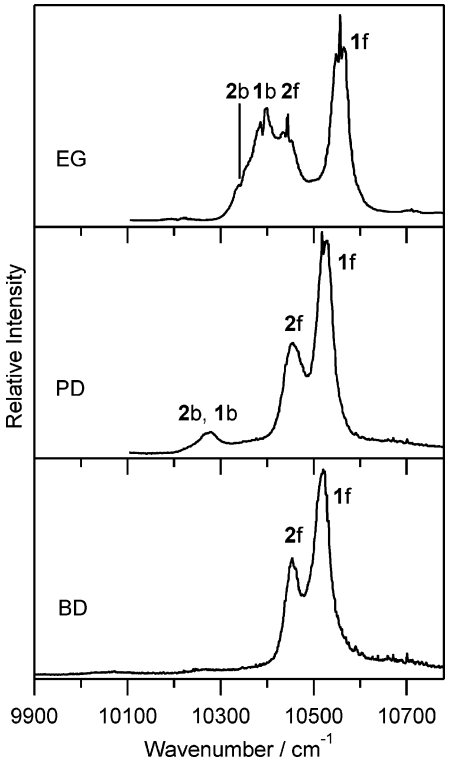

Figure 2. The vapor-phase overtone spectra of ethylene glycol (20 °C), 1,3-propanediol (20 °C), and 1,4-butanediol (40 °C) in the $\Delta v_{OH} = 3$ region.

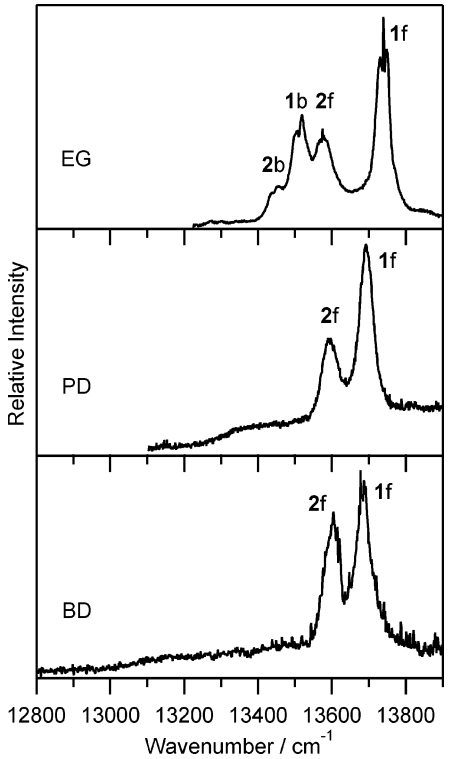

Figure 3. The vapor-phase overtone spectra of ethylene glycol (20 °C), 1,3-propanediol (20 °C), and 1,4-butanediol (40 °C) in the $\Delta v_{OH} = 4$ region.

cannot clearly distinguish two peaks corresponding to the two most stable conformers. This band is red-shifted relative to the free transitions of PD and to the bonded transitions of EG. Our calculations indicate that the **1**b and **2**b transitions of PD are separated by ~50 cm^{-1}, which is comparable to a typical OH-stretching bandwidth. In the $\Delta v_{OH} = 3$ BD spectrum, two very weak bands are observed at 10 070 and 10 256 cm^{-1}. The position of the band at 10 070 cm^{-1} agrees with the increasing red shift observed with the bonded transitions of EG and PD. The observed red shift is ~100 cm^{-1} greater than our QCISD-calculated red shift, as expected with the QCISD method,[13] and we tentatively assign the band at 10 070 cm^{-1} to the bonded transitions. The band at 10 256 cm^{-1} gets some of its intensity from weak transitions due to water vapor impurity in the sample and is less likely to be due to the **1**b and **2**b transitions. Our calculated **1**b and **2**b transitions of BD in the $\Delta v_{OH} = 3$ region are separated by only 15 cm^{-1}, so we would not expect to observe distinct bands for each transition.

In the $\Delta v_{OH} = 4$ EG spectrum, the bonded transitions of the two most stable conformers are again easily resolved. While bonded transitions could be observed in the $\Delta v_{OH} = 3$ PD spectrum, they cannot be clearly identified in the $\Delta v_{OH} = 4$ spectrum. However, there is a broad feature around approximately 13 400 cm^{-1}, which may be due, in part, to the bonded transitions. The $\Delta v_{OH} = 4$ region of BD appears similar to that of PD, with a broad band ranging from ~13 000 cm^{-1} to the location of the **2**f transition.

The region around 13 300 cm^{-1} may be complicated by the overlap of the **1**b and **2**b transitions with the less intense, albeit more numerous, methylene $\Delta v_{CH} = 5$ transitions, which are expected at these wavenumbers. For example, the methylene $\Delta v_{CH} = 5$ transition of propane is located at 13 302 cm^{-1} and the $\Delta v_{CH} = 4$ transition is at 10 914 cm^{-1}.[43] Thus, there is limited chance of overlap between CH-stretching and OH-stretching transitions in the $\Delta v_{OH} = 3$ spectra of Figure 2. The two lowest-energy conformers of PD (BD) combined yield a total of 12 (16) similar, but nonequivalent, methylene CH bonds, and their combined intensity could contribute to the broad feature observed in the $\Delta v_{OH} = 4$ spectra of PD and BD. However, the contribution from the methylene transitions is likely minimal, because the eight total nonequivalent methylene CH bonds in the two major conformers of EG are insignificant in the $\Delta v_{OH} = 4$ EG spectrum.

It is apparent from the observed spectra of PD and BD that the increase in intramolecular hydrogen bond strength plays a significant role in the OH_b-stretching transition intensities and/or bandwidths. Our anharmonic oscillator calculations have predicted the typical intensity trend for hydrogen bonding and provide good agreement with the higher-level calculations and observed spectra for EG.[13] Thus, we believe our intensity calculations for the second and third overtones are reasonable. Given that our calculations show the relative intensities of the OH_b-stretching overtone transitions in PD and BD are similar to those for EG, we attribute the observed "disappearance" of the OH_b-stretching transitions in PD and BD to bandwidth broadening.

We illustrate the effect of selectively increasing the width of the OH_b-stretching transitions of PD in Figure 4. For simplicity, we only include the two transitions of conformer **1**. The simulation is based on the observed **1**f and **1**b transition wavenumbers and our calculated relative intensity of approximately 1:2 for **1**b:**1**f in the $\Delta v_{OH} = 3$ region. A Lorentzian line shape with a full width at half-maximum (Γ_f) of 40 cm^{-1}, typically observed for OH-stretching overtones, was assigned to the **1**f transition and was kept fixed. The widths of the **1**b transitions (Γ_b) were chosen to be 40, 120, 240, and 360 cm^{-1}. The top spectrum in Figure 4 has equal widths of both transitions, and the resulting spectrum is similar to the observed spectrum of conformer **1** of EG. As the OH_b-stretching transition is broadened, it becomes more difficult to discern, similar to what we observe in our

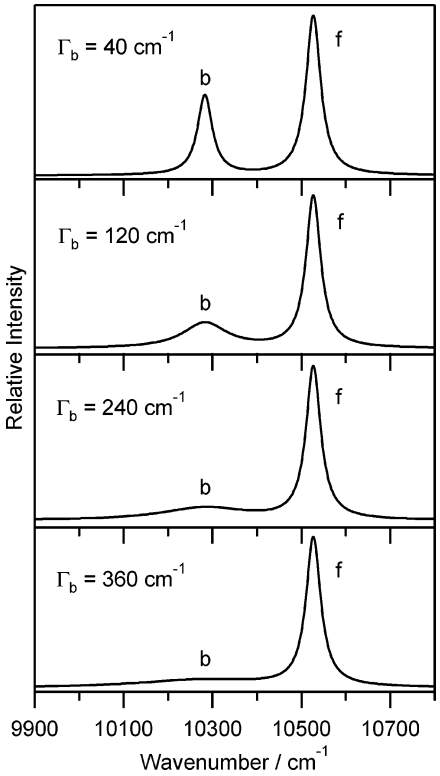

Figure 4. Broadening simulation of the bonded transitions of 1,3-propanediol conformer **1** in the $\Delta v_{OH} = 3$ region.

spectra in Figure 2 in the series EG to PD to BD. On the basis of these simulations, calculated intensities, and our measured spectra, we would estimate the width of the OH_b-stretching transition in the $\Delta v_{OH} = 3$ region of PD and BD to be approximately 120−240 cm^{-1} and approximately 360 cm^{-1} in the $\Delta v_{OH} = 4$ region. These results suggest that the increasing intramolecular hydrogen bond strength increases the width of the hydrogen-bonded OH_b-stretching overtone transitions. It also seems that the widths of the OH_b-stretching transitions increase from the $\Delta v_{OH} = 3$ to $\Delta v_{OH} = 4$ overtone.

We can speculate on the nature of this broadening. The observed fundamental donor-bonded OH-stretching transition of water dimer lacks resolvable rotational structure.[44] This has been attributed to lifetime broadening by predissociation or intramolecular vibrational energy redistribution (IVR) from the short-lived excited state.[44] The broadening observed for the bonded overtone transitions in PD and BD is likely analogous. The higher the overtone, the larger the excess energy above the hydrogen bond energy and the shorter its lifetime becomes. This should be significantly more efficient for excitation in the OH_b modes than in the OH_f modes. The additional vibrational modes in BD compared to PD and even more so EG increases the likelihood of so-called "doorway" states, which increases the efficiency of IVR.[45] The magnitude of the broadening observed in PD and BD is significant and offers an explanation for the difficulties associated with observing the OH_b-stretching overtones in, for example, water dimer.

It should be mentioned that an intrinsically low intensity of the OH_b-stretching transitions in PD and BD could also account for their disappearance and that our calculated intensities of the OH_b-stretching transitions are significantly overestimated. However, the required order of magnitude error in calculated intensity seems unlikely, given the agreement found for EG. Whether it is due to broadening or low intensity, the fact remains that the OH_b-stretching overtone transitions of PD and BD are very difficult to observe.

Conclusions

The vapor-phase OH-stretching overtone spectra of 1,3-propanediol and 1,4-butanediol have been recorded in the $\Delta v_{OH} = 3$ and 4 regions and compared to our previous spectra of ethylene glycol to investigate the effects of intramolecular hydrogen bonds. The room-temperature spectra of each diol are dominated by two conformers whose main geometrical difference is the dihedral angle of the "free" hydroxyl group.

Anharmonic oscillator calculations have been performed to simulate the spectra. The strong intensity increase of the OH_b-stretching fundamental and the excessive weakness in the first overtone, typical attributes of hydrogen bonds, have been calculated. The intensity of the OH_b-stretching transitions are calculated to steadily regain intensity at the third and higher overtones.

The increase in intramolecular hydrogen bond strength has a significant impact on the appearance of the OH_b-stretching transitions. The OH_b-stretching transitions appear to be increasingly broadened as the intramolecular hydrogen bond strength increases from 1,2-ethanediol, 1,3-propanediol, and 1,4-butanediol. We estimate that the widths of the OH_b-stretching overtone transitions of 1,3-propanediol and 1,4-butanediol are greater than 100 cm^{-1}. Due to this broadening, the OH_b-stretching overtone transitions of stronger intramolecular hydrogen bonds and hydrogen-bonded complexes are predicted to be more difficult to observe.

Acknowledgment. We acknowledge the Marsden Fund administered by the Royal Society of New Zealand for support, the Lasers and Applications Research Theme at the University of Otago for use of their computer facilities, and the University of Otago Research Committee, by means of the University of Otago Postgraduate Publishing Award.

Supporting Information Available: Calculated OH-stretching local-mode frequencies and anharmonicities of the three diols. Calculated OH-stretching peak positions and oscillator strengths. Measured peak positions in 1,3-propanediol and 1,4-butanediol in the $\Delta v_{OH} = 3$ and 4 overtones. This material is available free of charge via the Internet at http://pubs.acs.org.

References and Notes

(1) Vaida, V.; Kjaergaard, H. G.; Feierabend, K. J. *Int. Rev. Phys. Chem.* **2003**, *22*, 203-219.
(2) Vigasin, A. A., Slanina, Z., Eds. *Molecular Complexes in Earth's Planetary, Cometary and Interstellar Atmospheres*; World Scientific: River Edge, NJ, 1998.
(3) Vaida, V.; Daniel, J. S.; Kjaergaard, H. G.; Goss, L. M.; Tuck, A. F. *Q. J. R. Meteorol. Soc.* **2001**, *127*, 1627−1643.
(4) Daniel, J. S.; Solomon, S.; Kjaergaard, H. G.; Schofield, D. P. *Geophys. Res. Lett.* **2004**, *31*, L06118.
(5) Ptashnik, I. V.; Smith, K. M.; Shine, K. P.; Newnham, D. A. *Q. J. R. Meteorol. Soc.* **2004**, *130*, 2391−2408.
(6) Pfeilsticker, K.; Lotter, A.; Peters, C.; Bösch, H. *Science* **2003**, *300*, 2078−2080.
(7) Kassi, S.; Macko, P.; Naumenko, O.; Campargue, A. *Phys. Chem. Chem. Phys.* **2005**, *7*, 2460−2467.
(8) Suhm, M. A. *Science* **2004**, *304*, 823.
(9) Vaida, V.; Headrick, J. E. *J. Phys. Chem. A* **2000**, *104*, 5401−5412.
(10) Kuhn, L. P. *J. Am. Chem. Soc.* **1952**, *74*, 2492−2499.
(11) Tichy, M. *Adv. Org. Chem.* **1965**, *5*, 115−298.
(12) Buckley, P.; Giguère, P. A. *Can. J. Chem.* **1967**, *45*, 397−407.
(13) Howard, D. L.; Jørgensen, P.; Kjaergaard, H. G. *J. Am. Chem. Soc.* **2005**, *127*, 17096−17103.
(14) Klein, R. A. *J. Comput. Chem.* **2002**, *23*, 585−599.

(15) Mandado, M.; Graña, A. M.; Mosquera, R. A. *Phys. Chem. Chem. Phys.* **2004**, *6*, 4391−4396.
(16) Crittenden, D. L.; Thompson, K. C.; Jordan, M. J. T. *J. Phys. Chem. A* **2005**, *109*, 2971−2977.
(17) Vázquez, S.; Mosquera, R. A.; Rios, M. A.; Van Alsenoy, C. *THEOCHEM* **1988**, *181*, 149−167.
(18) Bultinck, P.; Andre, G.; Van de Vondel, D. *THEOCHEM* **1995**, *357*, 19−32.
(19) Shagidullin, R. R.; Chernova, A. V.; Plyamovatyi, A. K.; Shagidullin, R. R. *Bull. Acad. Sci. USSR, Div. Chem. Sci. (Engl. Transl.)* **1991**, *40*, 1993−1999.
(20) Kinneging, A. J.; Mom, V.; Mijlhoff, F. C.; Renes, G. H. *J. Mol. Struct.* **1982**, *82*, 271−275.
(21) Caminati, W.; Melandri, S.; Favero, P. G. *J. Mol. Spectrosc.* **1995**, *171*, 394−401.
(22) Fishman, E.; Chen, T. L. *Spectrochim. Acta, Part A* **1969**, *25*, 1231−1242.
(23) Shagidullin, R. R.; Chernova, A. V.; Shagidullin, R. R. *Russ. Chem. Bull.* **1993**, *42*, 1505−1510.
(24) Trætteberg, M.; Hedberg, K. *J. Am. Chem. Soc.* **1994**, *116*, 1382−1387.
(25) Hasanein, A. A.; Kovac, S. *J. Mol. Struct.* **1974**, *22*, 457−462.
(26) Jesus, A. J. L.; Rosado, M. T. S.; Leitão, M. L.; Redinha, J. S. *J. Phys. Chem. A* **2003**, *107*, 3891−3897.
(27) Cramer, C. J.; Truhlar, D. G. *J. Am. Chem. Soc.* **1994**, *116*, 3892−3900.
(28) Morantz, D. J.; Waite, M. S. *Spectrochim. Acta, Part A* **1971**, *27*, 1133−1137.
(29) Kjaergaard, H. G.; Turnbull, D. M.; Henry, B. R. *J. Chem. Phys.* **1993**, *99*, 9438−9452.
(30) Rong, Z.; Kjaergaard, H. G. *J. Phys. Chem. A* **2002**, *106*, 6242−6253.
(31) Wake, D. R.; Amer, N. M. *Appl. Phys. Lett.* **1979**, *34*, 379−381.
(32) Schattka, B. J.; Turnbull, D. M.; Kjaergaard, H. G.; Henry, B. R. *J. Phys. Chem.* **1995**, *99*, 6327−6332.
(33) Henry, B. R. *Acc. Chem. Res.* **1977**, *10*, 207−213.
(34) Jensen, P. *Mol. Phys.* **2000**, *98*, 1253−1285.
(35) Howard, D. L.; Kjaergaard, H. G. *J. Chem. Phys.* **2004**, *121*, 136−140.
(36) Low, G. R.; Kjaergaard, H. G. *J. Chem. Phys.* **1999**, *110*, 9104−9115.
(37) Werner, H.-J. et al. *MOLPRO*, version 2002.6, a package of ab initio programs; 2003.
(38) Pimentel, G. C.; McClellan, A. L. *The Hydrogen Bond*; W. H. Freeman: San Francisco, 1960.
(39) Iogansen, A. V. *Spectrochim. Acta, Part A* **1999**, *55*, 1585−1612.
(40) Hilbert, G. E.; Wulf, O. R.; Hendricks, S. B.; Liddel, U. *J. Am. Chem. Soc.* **1936**, *58*, 548−555.
(41) Di Paolo, T.; Bourdéron, C.; Sandorfy, C. *Can. J. Chem.* **1972**, *50*, 3161−3166.
(42) Kjaergaard, H. G.; Low, G. R.; Robinson, T. W.; Howard, D. L. *J. Phys. Chem. A* **2002**, *106*, 8955−8962.
(43) Kjaergaard, H. G.; Yu, H.; Schattka, B. J.; Henry, B. R.; Tarr, A. W. *J. Chem. Phys.* **1990**, *93*, 6239−6248.
(44) Huang, Z. S.; Miller, R. E. *J. Chem. Phys.* **1989**, *91*, 6613−6631.
(45) Nesbitt, D. J.; Field, R. W. *J. Phys. Chem.* **1996**, *100*, 12735−12756.